ESTIMATING IN-SITU RELATIVE PERMEABILITY AND CAPILLARY PRESSURE FROM MULTIPHYSICS WIRELINE MEASUREMENTS

Lin Liang, Lalitha Venkataramanan, Shihao Wang, Fábio C. Canesin, Vasileios-Marios Gkortsas, Koksal Cig, Aria Abubakar, and Tarek M. Habashy, Schlumberger

This paper was prepared for presentation at the SPWLA 59th Annual Logging Symposium held in London, UK, June 2-6, 2018.

ABSTRACT

We present a comprehensive workflow, in the presence of water-based-mud drilling fluids, to estimate in-situ relative permeability and capillary pressure curves by integrating multiphysics wireline measurements including array resistivity, dielectric, nuclear magnetic resonance (NMR), and formation testing and sampling data. Array resistivity logs are used for estimating the radial invasion profile and formation connate water saturation. Dielectric logs have shallow depths of investigation and hence are ideal for estimating residual oil saturation. Also, they provide vital information for determining Archie's parameters m and n. NMR data are used to estimate irreducible water saturation, and from the T_2 distribution, we can estimate a pore size distribution index (PSDI), which can help constrain the solution when inverting for relative permeability and capillary pressure curves. NMR data can also be input to the computation of a continuous permeability log that can be calibrated to permeabilities from cores or formation tests. Based on the derived PSDI, we can further narrow the physical bounds for Corey's exponents in the relative permeability model, i.e., the curvatures of relative permeability curves for the water phase and the oil phase. This workflow demonstrates an efficient method to obtain in-situ relative permeability and capillary pressure parameters, which can help fill the gap in reservoir modeling and simulation. The method has been successfully applied to different reservoir formations including shaly sands, carbonates, and unconsolidated siliciclastic reservoirs.

INTRODUCTION

Relative permeability and capillary pressure parameters play a vital role in reservoir modeling because they govern the spatial distribution and the flowing behavior of multiphase fluids, which coexist in the pores. However, efficiently obtaining representative relative permeability and capillary pressure parameters remains a long-standing challenge for the oil industry. To date, special core analysis (SCAL) in the laboratory is still the most-applied method for determining these parameters. This technique has obvious limitations. First, the length scale of the cores is usually much smaller than the scale required for reservoir modeling. Therefore, one upscaling step is needed to apply the core measurement to reservoir modeling, which is another challenging issue. Also, the process is costly and time-consuming. The experiments often require months or years to complete depending on resource availability and other logistics. Another critical issue is that the cores are often contaminated and altered and so do not represent the reservoir conditions. These factors make the relative permeabilities and capillary pressure measurements from SCAL unreliable for reservoir performance prediction. Fine-tuning on those parameters is often needed for history matching the production data before using them for forecasting.

It is of great advantage to develop a method to estimate relative permeability and capillary pressure parameters from in-situ downhole measurements so that the obtained parameters are under reservoir conditions, i.e., not subjected to contamination and alteration and ideally, with a more representative scale. Some work has been done in this direction in last decades. For example, Semmelbeck et al. (1995) and Ramakrishnan and Wilkinson (1999) integrated the mud-filtrate invasion process with array induction logs to characterize the relative permeability of the formation, which is more representative of an imbibition process. Zeybek et al. (2004) attempted to estimate relative permeability from the integration of array induction logs combined with pressure transient and water-cut measurements from a packer-probe wireline formation tester in a trial-and-error way. Alpak et al. (2004) developed a deterministic simultaneous joint inversion algorithm for deriving the relative permeability and capillary pressure curves from wireline array resistivity logs and formation testing data. Utilizing a stochastic optimization platform, Cig et al. (2014, 2015) developed a workflow to estimate relative permeability and capillary pressure from pressure transient and water-cut measurements from different types of wireline formation testers, which is more

representative of a drainage process although the imbibition process was honored by the invasion profile match.

We propose and develop a comprehensive workflow, in the presence of water-based-mud drilling fluids, to estimate in-situ relative permeability and capillary pressure curves by integrating multiphysics wireline measurements including array resistivity, dielectric, nuclear magnetic resonance (NMR), and formation testing and sampling data. The workflow is based on the framework developed previously in Liang et al. (2011) and Liang et al. (2017), which focused on the integration of array resistivity logs and formation testing and sampling data. As demonstrated in these works, the inverse problem becomes highly nonunique when inverting for relative permeability and capillary pressure from the formation testing and sampling data, which means multiple solutions could be obtained, with all of them being able to reconstruct the measurements almost equally well. Therefore, uncertainty is always a concern when using the workflow for field data processing.

In this work, we extend the above workflow by integrating additional measurements to effectively narrow down the solution space for the improved certainty of the interpretation. Array resistivity logs are widely used for estimating the radial invasion profile and formation connate water saturation. However, they are not sensitive to the residual oil saturation because these measurements are relatively deep whereas the movable oil is not completely displaced by mud-filtrate invasion. Dielectric logs have shallow depths of investigation and hence are ideal for estimating residual oil saturation. Also, they can be used to determine Archie's parameters m and n (Venkataramanan et. al., 2016). NMR data can be used to estimate the irreducible water saturation, and, from the T_2 distribution, we can estimate a pore size distribution index (PSDI), which can help constrain the solution when inverting for relative permeability and capillary pressure curves. NMR data can also be input to the computation of a continuous permeability log that can be calibrated to permeabilities from cores or formation tests. With that, we can build the near-wellbore reservoir model for simulation. Based on the derived PSDI, we can further narrow the physical bounds for Corey's exponents in the relative permeability model, i.e., the curvatures of relative permeability curves for the water phase and the oil phase.

Integration of multiphysics wireline measurements produces a reliable workflow for the determination of relative permeability and capillary pressure parameters with less uncertainty. The representative scale of these estimated parameters can be inches to feet, depending on the filtrate invasion depth. The time needed for data processing is negligible compared with laboratory core analysis experiments. Importantly, the relative permeability and capillary pressure parameters are estimated from downhole measurements, hence at in-situ reservoir conditions, which eliminates the need for further calibration or corrections for reservoir modeling.

This work demonstrates an efficient multiphysics integrated method to obtain in-situ relative permeability and capillary pressure data from a variety of wireline measurements, which can help fill the gap in reservoir modeling and simulation. The method has been successfully applied to different reservoir formations including shaly sands, carbonates, and unconsolidated siliciclastic reservoirs with heavy oil (Rashaid et. al., 2017).

GENERAL FRAMEWORK

We have previously developed a general framework for estimating in-situ relative permeability and capillary pressure from array-resistivity logs and formation testing and sampling data as shown in Figure 1 (Liang et al., 2017). In the workflow, a near-wellbore reservoir model is built based on all acquired data and prior knowledge. The mud-filtrate invasion process is modeled based on the actual job sequence. Wireline resistivity logging and formation testing and sampling processes can be simulated based on the scenario models generated from the mud-filtrate invasion simulation. The inversion process tunes the identified unknowns, which include parameters defining relative permeability and capillary pressure curves, until all the simulated data match the measurements. The inversion workflow is adaptive depending on the data availability and the parameters to be estimated. Usually, the invasion profile and the irreducible water saturation can be estimated from array-resistivity logs by coupling with the invasion simulation. This inverse problem is convex and can be solved reliably using deterministic optimization method such as Gauss-Newton. Inversion of relative permeability and capillary pressure relevant parameters from formation testing and sampling data is highly nonunique. Therefore, hybrid methods combining stochastic and deterministic methods are needed to ensure proper exploration of the solution space. More details about this workflow are provided in Liang et al. (2017).

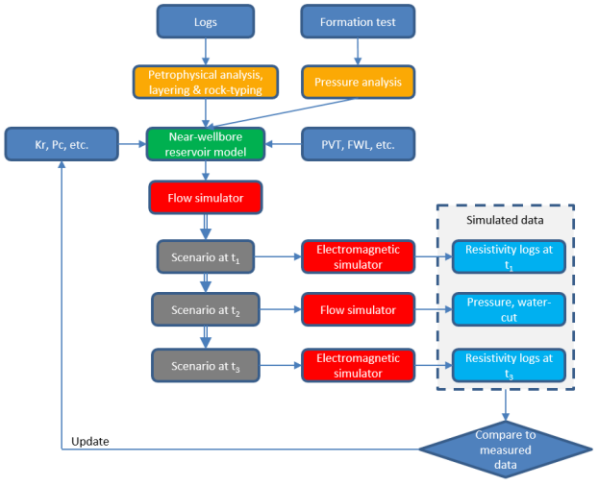

Fig.1 Framework for estimating relative permeability and capillary pressure from in-situ measurements.

RELATIVE PERMEABILITY AND CAPILLARY PRESSURE MODEL

Different formulations have been developed to describe the relative permeability and capillary pressure curves. We choose one widely used in reservoir modeling, i.e., the modified Brooks-Corey model (Lake, 1989):

$$S_w^* = \frac{S_w - S_{wr}}{1 - S_{wr} - S_{or}} \quad (1)$$

$$p_c(S_w) = p_{ce}(S_w^*)^{-\frac{1}{\lambda}} \quad (2)$$

$$k_{rw}(S_w) = k_{rw}^0(S_w^*)^{n_w} \quad (3)$$

$$k_{ro}(S_w) = k_{ro}^0(1 - S_w^*)^{n_o} \quad (4)$$

where k_{rw}^0 and k_{ro}^0 are the endpoint relative permeabilities for the water and oil phases, respectively; S_{wr} and S_{or} are the residual saturations for water and oil, respectively; n_w and n_o are Corey's exponents for water and oil, respectively; p_{ce} is the capillary entry pressure; and λ is the PSDI. Note that this formulation is more suitable for a water-wet system, but the formulation for relative permeability is still widely used for mixed-wet and oil-wet systems. Other formulas can be adopted easily whenever necessary. A typical set of relative permeability and capillary pressure curves from the modified Brooks-Corey model is shown in Figure 2, in which the parameters n_w, n_o, and λ are controlling the curvatures of water-phase relative permeability, oil-phase relative permeability, and capillary pressure curves, respectively. These curves are defined by eight parameters, as denoted in Figure 2. If we define the formation absolute permeability as the effective oil permeability at irreducible water saturation, k_{ro}^0 can be normalized to a unity, and we reduce the number of parameters to seven.

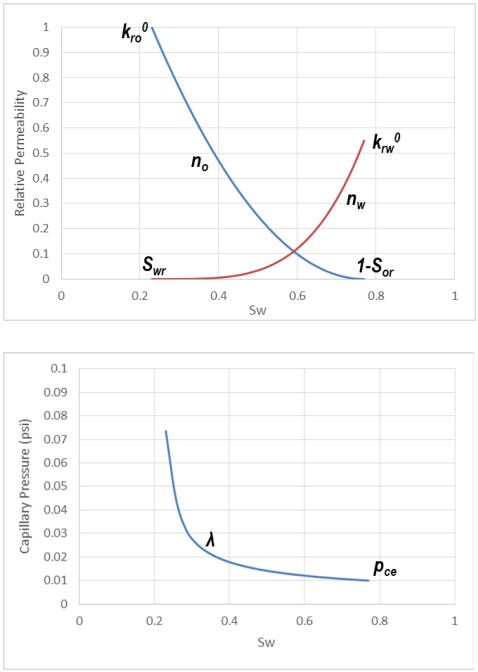

Fig.2 Relative permeability (top) and capillary pressure (bottom) curves defined by eight parameters.

WETTABILITY EFFECT ON RELATIVE PERMEABILITY AND CAPILLARY PRESSURE

Wettability refers to the tendency of one fluid to spread on or adhere to a solid surface in the presence of other immiscible fluids. It governs the spatial distribution of multiphase fluids in the rock pores and affects their movement through pores. For example, an oil-wet formation tends to hold more oil in its micropores and produce more water, whereas a water-wet formation is more favorable for producing oil. Different experiments have been designed and developed to qualify or quantify the wettability states of rock samples, for example, Amott (1959), Donaldson et al. (1969), Morrow (1990), Graue et al. (2002), and Derahman and Zahoor (2008).

Relative permeability and capillary pressure curves

contain information about the wettability state of the reservoir. Some general rules about reading wettability from relative permeability curves have been summarized in Craig (1971), Anderson (1987), and Falode and Manuel (2014). For example, as a rule of thumb, the irreducible water saturation is usually greater than 20% to 25% for a water-wet formation and less than 15% or even 10% for an oil-wet formation; the saturation at which oil and water relative permeabilities are equal is usually greater than 50% for water-wet and less than 50% for oil-wet; and the endpoint relative permeability of water phase generally less than 30% for water-wet and greater than 50% for oil-wet, based on the effective oil permeability at irreducible water saturation (Craig, 1971).

If the wettability state can be interpreted from other measurements such as cores or dielectric and NMR logs, theoretically it is possible to combine this information to help define the relative permeability and capillary pressure curves. For example, Huang et al. (1997) developed a model for relative permeability and capillary pressure interrelating with wettability indices and PSDI. But this is still a very limited study, and it is still very challenging for practical applications. However, this information can be used to narrow down the solution space by confining the range of Corey's exponents based on accepted heuristics. A water-wet formation has a lower ratio of k_{rw}^0/k_{ro}^0 in comparison to an oil wet formation. It has higher S_{wr} and, because oil is often trapped by the surrounding water, it also has a lower S_{or}. The shape of the relative permeabilities defined by n_w and n_o also varies with wettability. The nature of the variation of this shape is shown in Figure 3. In this illustration, the endpoint saturations and maximum relative permeabilities are fixed at 0.2 and 1, respectively.

In a water-wet scenario, water stays bound to the surface, and oil is expected to be in the middle of larger pores. Thus, it is characterized by a higher n_w and lower n_o in Equations 3 and 4. It has a higher oil relative permeability curve and a lower water relative permeability curve compared to an oil-wet rock, which is characterized by a lower n_w and higher n_o.

Goda and Behrenbuch (2004) provide a range of n_w and n_o for different scenarios of a rock wettability index. They showed that, for most cases, the values of both n_w and n_o are in the interval 2–8. Based on this range, a space of all possible solutions for relative permeability curves can be obtained, as illustrated as the shadowed regions (gray plus yellow) in Figure 4. If we can further confine the bounds of these two parameters, it is possible to narrow down the solution space as indicated by the gray regions, as an example of oil-wet scenario.

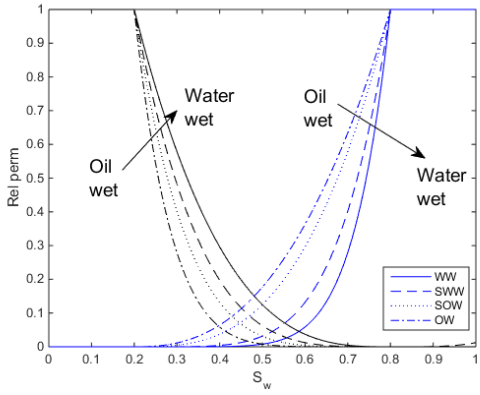

Fig.3 Effect of wettability on the shape of the relative permeability curves. WW, SWW, SOW, OW denotes water-wet, slightly water-wet, slightly oil-wet, and oil-wet, respectively.

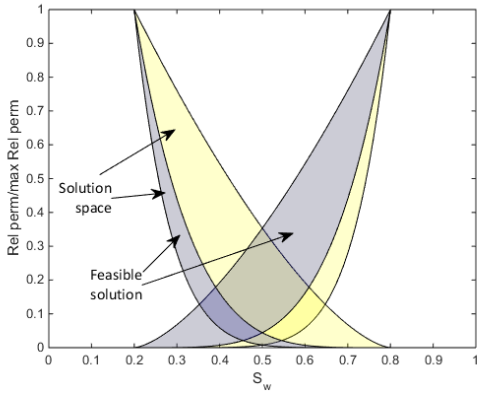

Fig.4 Using wettability information to narrow down the solution space. The gray plus yellow regions illustrate the full solution space if n_w and n_o are in the range of 2–8. The gray region illustrates a feasible solution region for an oil-wet formation, and we can narrow down the range of n_w and n_o values based on wettability state.

HETEROGENEITY EFFECT ON RELATIVE PERMEABILITY AND CAPILLARY PRESSURE

The relative permeability and capillary pressure curves are affected by the heterogeneity of the porous medium, λ, in Equations 1–4. From the Brooks and Corey (1964)

study of porous media, λ can take any positive value greater than zero; it is small for media with a wide range of pore sizes and large for media with a relatively uniform pore size. In their studies, λ was found to take values from 1.8 (silty loam) to 8 (glass bead pack). Today, λ is often found from mercury porosimetry data on cores. When cores are homogenous, with increasing pressure, there is almost a sharp change in saturation as mercury goes into many identical pores at the same time. On the other hand, when the cores are heterogenous, there is a gradual increase in mercury saturation with increasing pressure. Thus, using Equation 2, the slope of the mercury saturation versus pressure is used to obtain λ in the laboratory.

There are many models in the literature that predict relative permeability and capillary pressure curves. These models are either capillary or network models. Although there is variation between rocks, a modified Brooks-Corey method has been widely accepted for water-wet rocks, with $n_w = 3 + \frac{2}{\lambda}$ and $n_o = 1 + \frac{2}{\lambda}$ fitting the measured experimental brine/oil data reasonably well (Honarpour et al., 1986). The effect of λ on relative permeabilities is illustrated in Figure 5, where, as before, the endpoint saturations and maximum relative permeabilities are fixed. When λ is small (heterogenous cores), the fluid phases tend to be more tortuous, and the relative permeabilities are smaller than when λ is large (homogenous cores).

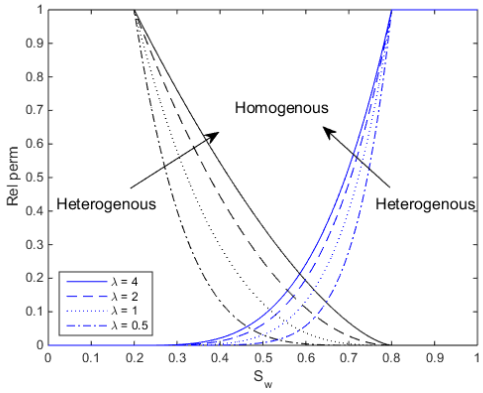

Fig.5 Effect of PSDI on the shape of the relative permeability curves for a water-wet rock.

ESTIMATE PORE SIZE DISTRIBUTION INDEX (λ) FROM NMR

An example of mercury porosimetry data on a core is shown in Figure 6A. As pressure is applied, mercury (Hg) fills the larger pores first. As pressure increases, Hg fills into smaller and smaller pores leading to increased saturation of Hg. The Brooks-Corey model in Equation 2 predicts a power-law variation of capillary pressure with normalized Hg saturation in Equation 1. This power-law behavior of data in Figure 6A is highlighted in Figure 6B, and a fit of Equation 2 to the data provides a $\lambda = 1.55$ and $P_{ce} = 10$ psi.

The NMR T_2 and its cumulative distribution for this 100% brine-saturated core is shown in Figure 6C. Under the assumption of a constant relaxivity and pore-body-to-throat ratio, the cumulative distribution has similar information to Hg data. A scaling factor $\kappa \triangleq P_c T_2$ is used to convert the cumulative T_2 distribution to a capillary pressure curve (Volokitin et al., 1999). In the absence of core data, a universally accepted rule of thumb for cores is $\kappa = 3$ psi-s. Converting the cumulative T_2 distribution to capillary pressure and the fit with the Brooks-Corey model is shown in Figure 6D and is seen to provide a very good fit to the Hg data with a $\lambda = 1.5$. In the literature, an optimal procedure for converting T_2 distribution to capillary pressure for a particular reservoir involves selecting core plugs, acquiring laboratory Hg and NMR measurements on 100% brine-saturated cores, and then finding either "an optimal" κ (Volokitin et al., 1999) or a capillary-pressure dependent κ (Altunbay et al., 2001).

Computing λ from NMR data from a partially oil/brine-saturated core is a challenging problem and requires many assumptions. From the analysis of the partially saturated data, a "best guess" T_2 distribution of the 100% brine-saturated data is obtained (Volokitin et al., 1999). This best guess is often based on observed correlation in cores between the bound fluid volume and the peak of the T_2 distribution of free water. A synthetic 100% brine-saturated T_2 distribution is obtained by applying a correction to the drainage T_2 distribution. This correction attempts to remove the T_2 distribution of the hydrocarbon and adds in the best-guess T_2 distribution of the free water. This method strongly relies on being able to guess the T_2 distribution of oil and water. We have developed an alternated method to estimate the pore size distribution index from partially saturated data. This method is based on a laboratory study of cores in different stages of brine/oil saturation and will be presented in a succeeding paper.

Once λ is computed from NMR T_2 data, approximate values of n_w and n_o are computed and used to derive upper and lower bounds for the inversion.

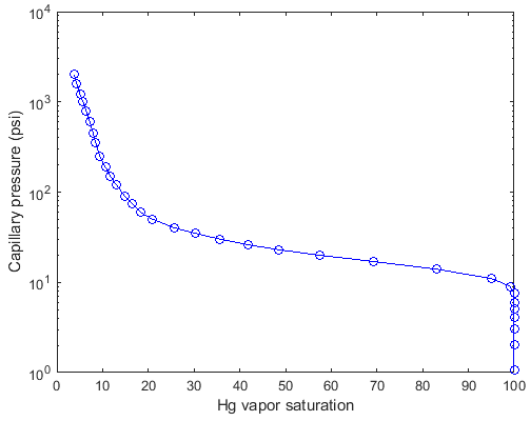

(A)

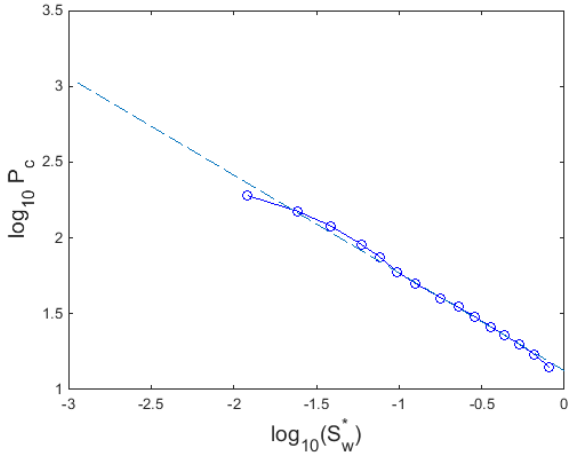

(B)

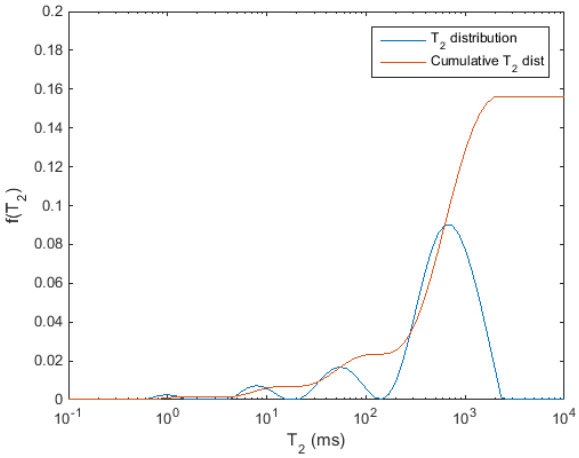

(C)

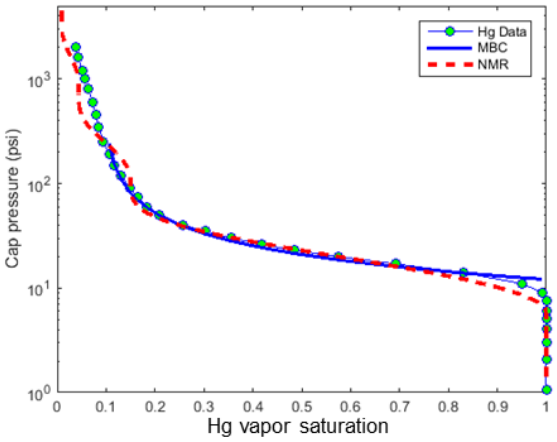

(D)

Fig.6 The first plot (6A) shows the mercury intrusion curve into the core. The same data plotted on a logarithmic axis and a normalized saturation are shown on the second plot (6B). The data are well fit by a modified Brooks-Corey (MBC) model with a λ of 1.55. The T_2 distribution (blue) and its cumulative (red) for this core are shown on the third plot (6C). Under the assumption that the core is well described across scales with a constant (although unknown) relaxivity and pore-body-to-throat ratio, the cumulative is also fit to a modified Brooks-Corey model. The data and the fit are shown on the last plot (6D).

NUMERICAL EXAMPLES

The integrated workflow has been successfully applied to a few field studies including the heavy oil field in Kuwait and a carbonate oil field in Saudi Arabia. In this paper, we demonstrate the concept using a numerical example. The structure of the model is based on the numerical example used in Liang et al. (2017) with modifications to some parameters, especially for facies 0, which are listed in Table 1. In this example, the formation model is composed of eight layers, which can be categorized into three facies. Array induction logging is carried out for the entire depth interval two days after drilling, immediately followed by dual-packer formation testing and sampling in the interval 5,021.67 to 5,025 ft with an offset probe set at 5,017 ft for observing the pressure transient. An in-situ fluid analyzer is used to record the water-cut information (WCT) from the dual-packer pumping.

Table 1: Input parameters for the numerical example. Q, $\emptyset$, k_h, k_v/k_h, and s_d denote average invasion rate, porosity, horizontal permeability, permeability anisotropy, and damage skin factor, respectively.

Parameters	Facies 0	Facies 1	Facies 2
Q (rb/day/ft)	0.05	0.015	0.005
$\emptyset$	0.25	0.2	0.15
k_h (md)	300	80	5
k_v/k_h	0.25	0.1	0.05
S_{wr}	0.1	0.2	0.25
S_{or}	0.15	0.2	0.25
k_{rw}^0	0.3	0.4	0.6
k_{ro}^0	1.0	1.0	1.0
n_w	5.5	4.7	4.0
n_o	3.5	2.7	2.3
λ	0.8	1.2	1.5
p_{ce} (psi)	0.67	0.89	1.6
s_d	0.15	0.1	0.05
m	1.8	1.9	2.0
n	1.9	2.0	2.1

Following the similar workflow described in Liang et al. (2017), we first invert the array resistivity logs using the deterministic method, then invert the formation testing and sampling data using the Monte-Carlo-Gauss-Newton method. From the first step inversion, we obtain invasion rates for each layer and the irreducible water saturation for each facies as shown in Figure 7 (Hu et al., 2017). The inverted residual oil saturations usually deviate from the true values due to the weak sensitivity of array resistivity logs to the shallow region of the formation. Hence, it is necessary to determine the residual oil saturation from other sources such as dielectric logs, which have an investigation of 1 to 4 inches into the formation. In the second step, assuming the residual oil saturations have been obtained from dielectric logs, we invert for a list of unknown parameters for the target layer, where the formation testing and sampling is performed, from the recorded pressure transient and sampling data. As stated, this inverse problem is highly nonunique. To avoid trapping in a local minimum, we start from 48 initial models generated by random sampling from normal distributions and run Gauss-Newton optimizations to search for the best solution from each initial model to fit the measured pressure and water cut data. In this example, the target layer is the sixth layer from the top, as shown in the left track of Figure 7, which belongs to facies 0, colored in blue. The inverted relative permeability and capillary pressure curves for facies 0 are shown in Figure 8. It shows that there are multiple solutions (the top 12 solutions are plotted) fitting the formation testing and sampling data almost equally well. Figure 9 shows the comparison between the measurements and the dual packer pressure and water-cut data reconstructed from different solutions. The discrepancies between the results from different solutions are visually negligible and overlap with measurements. The pressure recorded by the probe is not shown here because it shares the same observation, i.e., almost perfect data fitting from multiple solutions. Figure 10 plots all inverted parameters with error bars shown in red presenting the variations from the selected top 12 solutions. Horizontal green lines denote the corresponding true value of each parameter used in the synthetic model. The top axis shows the physical bounds of each parameter we employed during the inversion. Here we used very loose bounds for the parameters n_w,n_o, and λ assuming we do not have any prior information from other sources. According to the recommendation from experimental data in Goda and Behrenbuch (2004), the ranges of both n_w and n_o can be confined in a range 2-8 for most cases.

If we can estimate the PSDI from NMR data, the physical bounds of λ, n_w, and $n_o$can be narrowed down for the inversion. Here we assume that the range of λ can be narrowed down to the range 0.7–0.9, based on the computation from the relationship between the Corey's exponents and PSDI for a water-wet case; n_w could be limited to ~4.5–5.8; and n_o can be limited to ~3.3–4. The new inversion results (top 12 solutions) are shown in Figure 11. Figure 12 plots all inverted parameters with the applied physical bounds during inversion shown on the top axis. As expected, the solutions are still nonunique, but have been effectively narrowed down.

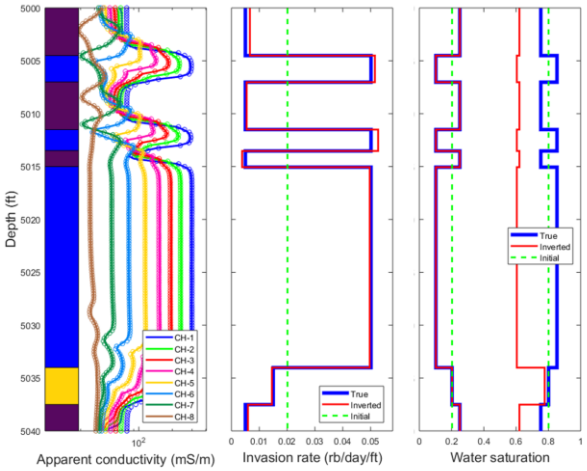

Fig.7 Inversion of array resistivity logs constrained by fluid flow. The first track shows the actual facies model and data-fitting on array resistivity logs. The second track shows the inverted invasion rates compared to the truth. The third track shows inverted irreducible water saturation compared to the truth (left part) and the inverted residual oil saturation compared to the true values (right part).

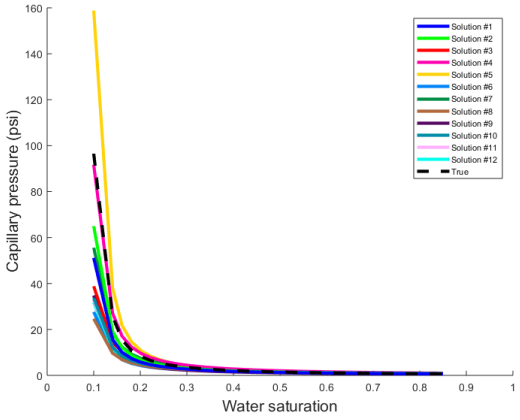

Fig.8 Inverted relative permeability and capillary pressure for facies 0 using loose bounds compared to the true model. Multiple solutions are shown in different colors except that the true model is shown with the black dashed line.

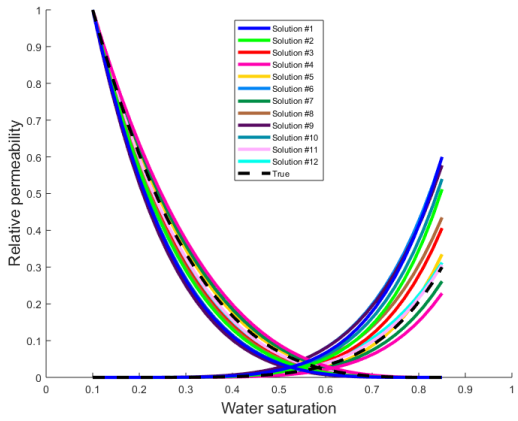

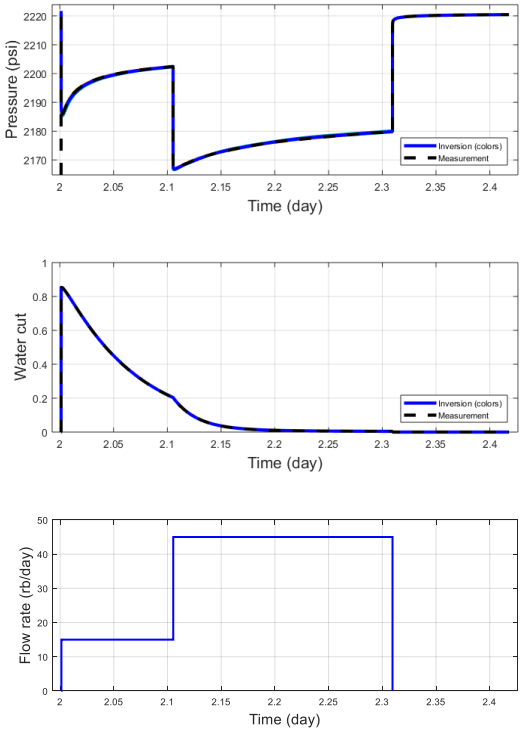

Fig.9 Comparison of reconstructed sink-pressure from 12 solutions to the measured sink pressure (top) and reconstructed water cut from 12 solutions to the measured water cut (middle). The data are visually identical. The bottom plot shows the flow rate during the formation testing and sampling process.

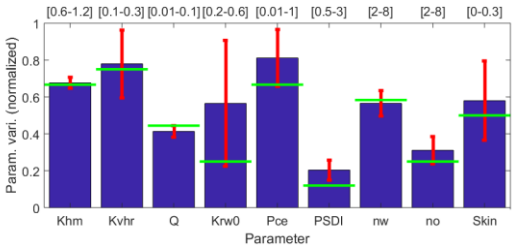

Fig.10 Bar plot for all inverted parameters normalized to [0-1] by the corresponding physical bounds shown on the top axis. The horizontal green lines represent the true values of parameters used for generating the synthetic data. Khm , $Kvhr$, and $Krw0$ denote horizontal permeability multiplier, permeability anisotropy ratio, and endpoint relative permeability for water phase, respectively.

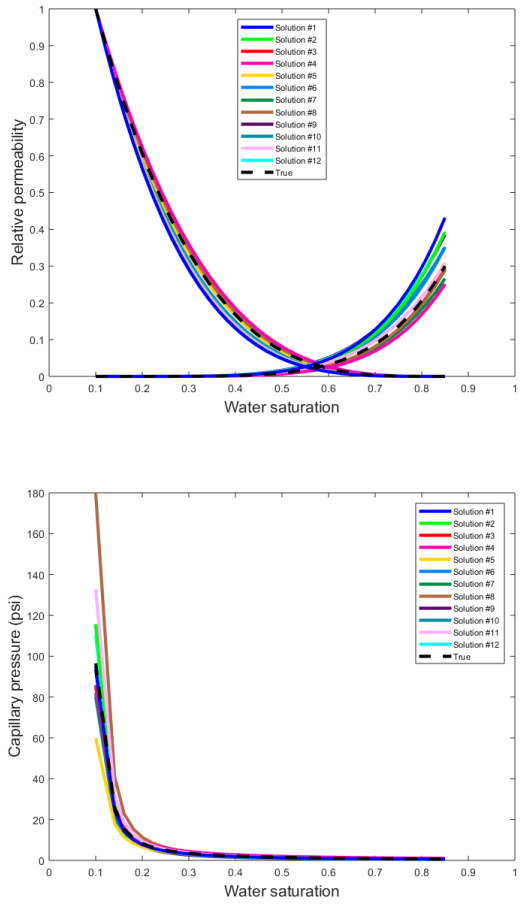

Fig.11 Inverted relative permeability and capillary pressure for facies 0 using confined bounds compared to the true model. Multiple solutions are shown in different colors except that the true model is shown with the black dashed line.

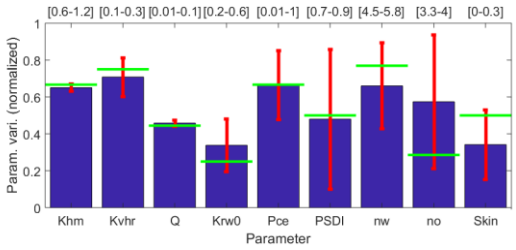

Fig.12 Bar plot for all inverted parameters normalized to 0–1 by the corresponding physical bounds shown on the top axis. The horizontal green lines represent the true values of parameters used for generating the synthetic data.

CONCLUSION

We developed an integrated workflow for estimating in-situ relative permeability and capillary pressure curves from the wireline measurements including a variety of well logs and the formation testing and sampling data. Among the data, array resistivity logs characterize the invasion profile and the irreducible water saturation. The dielectric log provides information on residual oil saturation and, by combining with NMR logs, provides insight on Archie's parameters *m* and *n*. The NMR log can be used to estimate PSDI, which could be used to narrow down the feasible range of a few parameters including Corey's exponents n_w and n_o . With these parameters being confined a priori, we can effectively reduce the solution space and the uncertainty in the interpretation. This workflow has been applied to a few field data studies including the heavy oil unconsolidated sandstone in Kuwait and the carbonates in Saudi Arabia. It needs to be noted that, although the water-based-mud invasion refers to an imbibition process, the inverted relative permeability and capillary pressure curves are dominated by the drainage process induced by the formation testing and sampling operation. The hysteresis effect has not been taken into account in this study.

REFERENCES

Alpak, F.O., Torres-Verdín, C., Habashy, T.M., and Sephernoori, K., 2004. Simultaneous estimation of in-situ multiphase petrophysical properties of rock formations from wireline formation tester and induction logging measurements. SPE Annual Technical Conference and Exhibition. SPE-90960-MS.

Altunbay, M., Martain, R., and Robinson, M., 2001. Capillary pressure data from NMR logs and its implications on field economics, SPE Annual Technical Conference and Exhibition. SPE-71703-MS.

Amott, E., 1959. Observations relating to the wettability of porous rock. Trans. AIME, vol. 216, pp. 156–162.

Anderson, W.G., 1987. Wettability literature survey – Part 5: The effects of wettability on relative permeability. Journal of Petroleum Technology, vol. 39, pp. 1,453–1,468.

Brooks, R.H. and Corey, A.T., 1964. Hydraulic properties of porous media. Hydrology Papers, No. 3, Colorado State University, Fort Collins, Colorado.

Cig, K., Ayan, C., Kristensen, M., Liang, L., El Battawy, A., Elshahawi, H., Ramaswami, S., Mackay, E., et al., 2015. Inversion of wireline formation tester data to estimate in-situ relative permeability and capillary pressure. Abu Dhabi International Petroleum Exhibition and Conference. SPE-177451-MS.

Cig, K., Ayan, C., Kristensen, M. R., Mackay, E. J., Elbekshi, A., et al., 2014. A novel methodology for estimation of multiphase flow properties from sampling data of wireline formation tester. In SPE Annual Technical Conference and Exhibition. SPE-70648-MS.

Craig, F.F., 1971. The reservoir engineering aspects of waterflooding. Monograph Series, SPE, Rchardson, TX.

Derahman, M.N. and Zahoor, M.K., 2008. Prediction and estimation of capillary pressure for wettability and wettability variations within reservoir. Proceedings of the 13th Abu Dhabi International Petroleum Exhibition and Conference, pp. 591–609.

Donaldson, E.C., Lorenz, P.B. and Thomas, R.D., 1969. Wettability determination and its effect on recovery efficiency. Soc. Petrol. Engr. J., vol. 9, no. 1, pp. 13–20.

Falode, O. and Manuel, E., 2014. Wettability effects on capillary pressure, relative permeability, and irreducible saturation using porous plate. Journal of Petroleum Engineering, vol. 2014. Article ID 465418.

Goda, H. M. and Behrenbuch, P., 2004. Using a modified Brooks Corey model to study oil-water relative permeability for diverse pore structures. SPE Asia Pacific Oil and Gas Conference and Exhibition. SPE-88538-MS.

Graue, A., Aspenes, E., BognØ, T., Moe, R.W., and Ramsdal, J., 2002. Alteration of wettability and wettability heterogeneity. Journal of Petroleum Science and Engineering, vol. 33, no. 1–3, pp. 3–17.

Honarpour, M., Koederitz, L., and Harvey, A.H., 1986. Relative permeability of petroleum reservoirs, CRC Press.

Hu, Y., Wang, G.L., Liang, L., and Abubakar, A., 2017. Estimation of reservoir parameters from inversion of triaxial induction data constrained by mud-filtrate invasion modeling. IEEE Journal on Multiscale and Multiphysics Computational Techniques, vol. 2, pp. 228–236.

Huang, D., Honarpour, M.M., and Al-Hussainy, R., 1997. An improved model for relative permeability and capillary pressure incorporating wettability. SCA International Symposium Calgary, Canada.

Liang, L., Abubakar, A., and Habashy, T. M., 2011. Estimating petrophysical parameters and average mud-filtrate invasion rates using joint inversion of induction logging and pressure transient data. Geophysics, vol. 76, no. 2, pp. E21–E34.

Liang, L., Zhu, J., Wang, F., Chen, J., Habashy, T. M., and Abubakar, A., 2017. In-situ estimation of relative permeability and capillary pressure from the joint inversion of array resistivity and formation test data. SPE Annual Technical Conference and Exhibition. SPE-187193-MS.

Morrow, N.R., 1990. Wettability and its effect on oil recovery. Journal of Petroleum Technology, vol. 42, no. 12, pp. 1476–1484.

Ramakrishnan, T. S. and Wilkinson, D. J., 1999. Water-cut and fractional flow logs from array-induction measurements. SPE Reservoir Evaluation & Engineering, vol. 2, no. 1, 85–94.

Rashaid, M., Al-Ibrahim, M., Van Steene, M., Ayyad, H., Friha, A., Liang, L., Cig, K., Ayan, C., Habashy, T., Cherian, J., 2017. Application of a new methodology for in-situ evaluation of relative permeability and capillary pressure in the Ahmadi Field of Greater Burgan, Kuwait. SPE Middle East Oil & Gas Show and Conference, SPE-183868-MS.

Semmelbeck, M. E., Dewan, J. T., and Holditch, S. A.,

1995. Invasion-based method for estimating permeability from logs. SPE Annual Technical Conference and Exhibition. SPE-30581-MS.

Venkataramanan, L., Donadille, J.M., Reeder, S.L., Van Steene, M., Gkortsas, V.-M., Fellah, K., Ramsdell, D., Al-Rubaiyea, J.A., Al-Ajmi, F.A., Al-Houli, M., Wilkinson, P., Bajunaid, H., 2016. A new method to estimate cementation and saturation exponents from dielectric dispersion data. SPE Annual Technical Conference and Exhibition. SPE-181451-MS.

Volokitin, Y, Looyestijn, W., Slijkerman, W., and Hofman, J., 1999. Constructing capillary pressure curves from NMR log data in the presence of hydrocarbons, paper KKK, SPWLA.

Zeybek, M., Ramakrishnan, T., AI-Otaibi, S., Salamy, S., and Kuchuk, F., 2004. Estimating multiphase-flow properties from dualpacker formation-tester interval tests and openhole array resistivity measurement. SPE Reservoir Evaluation & Engineering, vol. 7, no. 1, 40–46.

ABOUT THE AUTHORS

Lin Liang is a Principal Research Scientist and Program Manager in Schlumberger-Doll Research Center in Cambridge, Massachusetts. He works on multiphysics modeling and inversion for hydrocarbon exploration and reservoir characterization and reservoir simulation and history matching problems, as well as the application of data science and machine learning techniques to exploration and field development. Liang holds a BS degree in fluid machinery and fluid engineering from Tsinghua University and a Ph.D. degree in environmental science from Peking University. Liang joined Schlumberger in 2002. He is a member of SEG, SPE, and SPWLA.

Lalitha Venkataramanan is a Scientific Advisor in the Math and Modeling department at Schlumberger Doll Research, Boston. Her current interests include mathematical modeling and inversion, optimization, probability and stochastic processes. Trained as an Electrical Engineer, she obtained her M.S and PhD degrees from Yale University in 1998.

Shihao Wang is a PHD candidate in Colorado School of Mines. His recent work focused on numerical simulation of the multiphysical processes in petroleum reservoirs. He has authored more than 10 peer-reviewed papers. He has one-year field experience of hydraulic fracturing.

Fábio C. Canesin is a Research Engineer at Schlumberger Brazil Research and Geoengineering Center (BRGC) in Rio de Janeiro. He joined BRGC in 2012. His recent work focused on numerical analysis and software development and high-performance computing. He received BEng. in mechanical engineering from Federal University of Santa Catarina.

Vasileios-Marios Gkortsas is a Research Scientist in Schlumberger-Doll Research (SDR) at Cambridge, Massachusetts, USA. He joined SDR in 2013. His work focuses on the quantitative evaluation of conventional and unconventional formations from multi-physics measurements and on the application of machine learning techniques for cement evaluation. Dr. Gkortsas hold an S.M. in Applied Physics from Harvard University and a Ph.D. in Electrical Engineering and Computer Science from MIT.

Koksal Cig is a Reservoir Engineering Advisor for Schlumberger. He received a BS degree from the Istanbul Technical University and an MS degree from the University of Texas at Austin and a Ph.D. degree from the Heriot-Watt University, all in Petroleum Engineering. He joined Schlumberger in 1997 and he has worked as a reservoir engineer and a cased hole log analyst in various countries. Recently he supports wireline formation tester applications in several Middle Eastern countries.

Aria Abubakar received an MSc degree (cum laude) in electrical engineering and a PhD degree (cum laude) in technical sciences, both from the Delft University of Technology, in 1997 and 2000, respectively. From September 2000 until February 2003, he was a researcher with the Laboratory of Electromagnetic Research and Section of Applied Geophysics, Delft University of Technology. He joined Schlumberger-Doll Research Center in 2003 and his last position there was a Scientific Advisor and the Program Manager of Multi-Physics Modeling and Inversion program. Since 2013, he has been the Interpretation Engineering Manager and Scientific Advisor at Schlumberger Houston Formation Evaluation in Sugar Land, Texas.

At present, his main research activities include solving forward and inverse problems in acoustics, electromagnetics, and elastodynamics. He is currently the Associate Editor of Geophysics. He was the 2014 SEG North America Honorary Lecturer. He holds 14 US patents/patent applications and has published 1 book, 4 book chapters, over 75 scientific articles in refereed journals, 155 conference proceedings papers, and 50 conference abstracts. He has also presented over 300 invited and contributed talks in international conferences and institutes/universities.

Tarek Habashy has a Ph.D. from MIT in electrical engineering. He joined Schlumberger-Doll Research Center (SDR) in 1983 where he held a number of scientific and managerial positions and is currently a Schlumberger Fellow. From February 2012 to October 2016, he was the Managing Director of SDR. His main accomplishments are in R&D related to exploration and characterization technologies for the oil and gas industry. Throughout his career, he has conducted research in electromagnetic waves and fields, inverse scattering theory, multiphysics inversion, antenna theory and design, dielectric and resistivity logging tools and techniques, mixed boundary value problems, and numerical methods. He is a former editor of *Radio Science* and is a member of the editorial boards of *Wave Motion*, *Inverse Problems*, and *Progress in Electromagnetic Research*. He is a Fellow of the IoP and IEEE. He holds 50 US patents, has published 10 book chapters, and has written over 150 scientific papers and 150 proceedings papers.